Jurnal Kejuruteraan 35(3) 2023: 625-634
https://doi.org/10.17576/jkukm-2023-35(3)-10

The Performance of Isolated Half-Scissor Like Elements Mechanism Under Compression Axial Load

Chai Teck Jung[a*], Tan Cher Siang[b] & Koh Heng Boon[c]

[a]*Department of Civil Engineering, Politeknik Sultan Idris Shah, Malaysia.*
[b]*Faculty of Civil Engineering, Universiti Teknologi Malaysia, Malaysia*
[c] *Faculty of Civil Engineering and Built Environment, Universiti Tun Hussein Onn Malaysia, Malaysia*

**Corresponding author: tjchai@psis.edu.my*

Received 5 August 2022, Received in revised form 25 November 2022
Accepted 14 December 2022, Available online 30 May 2023

ABSTRACT

Half-Scissor Like Elements (H-SLEs) deployable mechanism is the prefab scissor based structural mechanism consists of two bars with bolted connection to enable structure change shape. An experimental investigation on the isolated H-SLEs deployable mechanism under compression axial load was presented. A total of twelve specimens were fabricated in two series with six specimens each series were tested on their strength and stability at deployed configuration. The test specimens in series 1 mm thick C75 section were namely S1, S2, S3, S4, S5 and S6 while series 0.75 mm thick C 75 section were namely S7, S8, S9, S10, S11 and S12. The test specimens consist of C 75 and C 100 section which connected with M6, M8 and M10 bolt in grade 8.8. The compression axial load was applied at the center of 3 mm thick loading platform. The experimental results obtained indicated that four types of failure modes observed, i.e. bolt bending failure, section bearing failure, member buckling failure and instability due to horizontal displacement at mid-height of H-SLEs deployable mechanism (Bolted joint area). Among these failure modes, bolt bending failure was dominated the overall structure stability and impacts others failure modes indirectly while section thickness has impacted the buckling and bearing failure. The ultimate load capacity over BS EN 1993 design bearing resistance ratio obtained for M10 bolt was satisfactory. Besides, twisted effect observed during load applied also contributed to the failure modes identified. Thus, the H-SLEs deployable mechanism with stiffener with M10 bolt connection is necessary for future research in the application of spatial deployable structure purposes.

Keywords: Half Scissor-Like Elements (H-SLEs); deployable mechanism; stability; bolt bending failure; bearing capacity; ultimate load

INTRODUCTION

The structures transformation to designate architectural function required a mobility called deployable mechanism. Deployable mechanism used as structural applications is the part of the load bearing structure itself. Scissor-Like Elements (SLEs) mechanism based on scissor principle was the simple and widely used deployable mechanism since first introduced in 1961 (Esther 2015). SLEs consists of two straight bars connected at their intermediate point with pivot and allow geometric transformations (Maden et al. 2011). The basic unit of translational SLEs mechanism is showed in Figure 1 (Gantes et al. 1989; Tagawa et al. 2015). The current prefabricated fast build construction industry has faced the logistic and space storage issues in achieving productivity. Notice that transformable technique by using SLEs deployable mechanism will help to solve these problems. Thus, the SLEs mechanism with various design and materials used to form the structure has become a hot topic to be investigated to provide a stiff and stable structure.

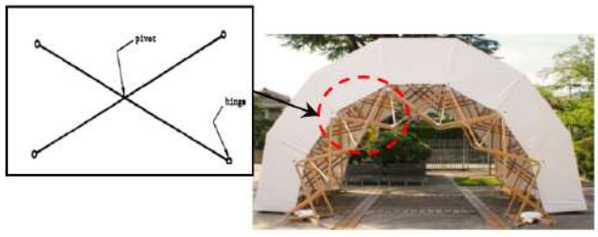

FIGURE 1. Scissor-like elements (SLEs) mechanism for deployable structure application

The previous research conducted on SLEs mechanism has explored and determined the solutions in improving the existing system to become a stable, reliable, stiff, and achieved deployability of the structures. Gantes et al. (1989) has explored the SLEs mechanism deployable structure system stability using computer design tool with parametric analysis verification. Others related studies on SLEs mechanism deployable structures included snap through effect (Friedman et al. 2013), variation of SLEs mechanism deployable structures perimeter (You et al.

1997), deployability of the structures (Kwan et al. 1993), reliability in SLEs mechanism deployed geometry, stiffness, and their function (Andrea et al. 2013), proposed design and alignment concept for SLEs deployable structures development (Roovers & Temmerman 2017), experimental and numerical studies for self-locking ability (Zhao et al. 2020) etc.

However, the experimental studies on isolated SLEs deployable mechanism at deployed configuration as compression member was less since it always investigated as structure in global. The SLEs mechanism at deployed configuration was behaving as column subjected to compression axial load. The compression member possesses the high risk to create instability problem when load applied. This was due to the nature of compression member at vertical state will suddenly bow at their mid-height and caused buckling failure (Megson, 2005). Therefore, the individual behaviour of the SLEs mechanism as load bearing structure must be determined. In 2017, Li et al has investigated the SLEs column stability under gravity load using energy theory. The additional restraint provided will improved column axial stiffness and postponed snap through buckling effect of the SLEs mechanism (Raskin & Roorda, 1999). Besides, the deployed SLEs mechanism must be able to sustain applied load (Hu et al. 2013) as load bearing structure to ensure the overall stability of the structure.

Therefore, this paper establishes a novel experimental work to investigate the behaviours of isolated Half Scissor-Like Elements (H-SLEs) deployable mechanism under compression axial load. At the end of the experimental work, the critical parameters, suitable section and connection size and failure modes were determined and discussed.

METHODOLOGY

SECTION AND GEOMETRY PROPERTIES

A total of twelve numbers of isolated H-SLEs deployable mechanism behave as column were built by cold-formed C-Section (CFCS) with bolted connection. Among these twelve samples, all outer section size is same, which is C100×51×12×1.6 mm thick while inner section sizes are six numbers of C75×38×8×0.75mm thick and six numbers of C75×38×8×1mm thick. The bolt size used for the connection between C-section (Inner and Outer section) were M6, M8 and M10 with grade 8.8. The twelve samples identification were tabulated in Table 1.

The section capacity used was calculated according to the BS EN 1993-1-1 (2005), BS EN 1993-1-3 (2006) and BS EN 1993 - 1 – 8 (2005). The actual average yield strengths found from tensile test were 550 MPa for 0.75 mm and 1 mm thick CFCS, 1.6 mm thick CFCS was 518 MPa and 589 MPa for 12 mm diameter rebar. Therefore, the section capacity was designed using steel strength of 500 MPa for CFCS and rebar to ensure quality assurance. The material and section properties are tabulated in Table 2.

TABLE 1. Isolated H-SLEs deployable mechanism identification

No	ID	C-Section Dimension	Bolt Dia (mm)	Height, (mm)
1	S1	C75×38×8×1 mm thk. & C100×51×12×1.6 mm thk.	6	1158
2	S2	C75×38×8×1 mm thk. & C100×51×12×1.6 mm thk.	6	1158
3	S3	C75×38×8×1 mm thk. & C100×51×12×1.6 mm thk.	8	1158
4	S4	C75×38×8×1 mm thk. & C100×51×12×1.6 mm thk.	8	1158
5	S5	C75×38×8×1 mm thk. & C100×51×12×1.6 mm thk.	10	1158
6	S6	C75×38×8×1 mm thk. & C100×51×12×1.6 mm thk.	10	1158
7	S7	C75×38×8×0.75 mm thk. & C100×51×12×1.6 mm thk.	10	1158
8	S8	C75×38×8×0.75 mm thk. & C100×51×12×1.6 mm thk.	10	1158
9	S9	C75×38×8×0.75 mm thk. & C100×51×12×1.6 mm thk.	8	1158
10	S10	C75×38×8×0.75 mm thk. & C100×51×12×1.6 mm thk.	8	1158
11	S11	C75×38×8×0.75 mm thk. & C100×51×12×1.6 mm thk.	6	1158
12	S12	C75×38×8×0.75 mm thk. & C100×51×12×1.6 mm thk.	6	1158

TABLE 2. Section and material properties.

Spec.	t mm	A mm^2	I_z mm^4	I_y mm^4	W_y mm^3	W_z mm^3	f_y MPa	f_u MPa	E MPa
C 75×38×8	0.75	113.26	21678	103222	2941	906	550	593	208000
C 75×38×8	1	152.17	28658	137630	3936	1204	550	636	210500
C100×50×12	1.6	332.5	110855	533401	11305	3540	518	571	194000
Reinforcement Bar									
Spec.	Ø (mm)		A (mm^2)	f_y (MPa)		f_u (MPa)		E (MPa)	
Ribbed Bar	12		113.1	589		672		233000	

EXPERIMENTAL CONFIGURATION AND APPARATUS SETUP

There were total of two Linear Variable Displacement Transducers (LVDTs) used to measure the displacements at vertical (Figure. 2c. iv) and horizontal direction (Figure. 2b) respectively. The top and intermediate level of the H-SLEs deployable mechanism was restrained by Y-12 rebar to the main test frame while base bolted to ground with M10 bolt (Figure. 2a). One 6 mm gauge length strain gauge (120 Ω) was stickled to the C75 section at bolt connection area (Figure. 2b). The specimen under compression axial load test configuration was showed in Figure. 2a. The type of test arrangement employed in this study was the twelve H-SLEs mechanism will displace horizontally due to compression axial load applied. The point load was applied at the middle top of 200 mm x 200 mm x 20 mm thick steel plate to distribute the point load to the H-SLEs deployable mechanism (Figure. 2c. iv). The hydraulic jet with 300 kN load cell was used to apply load (Figure. 2c. iv).

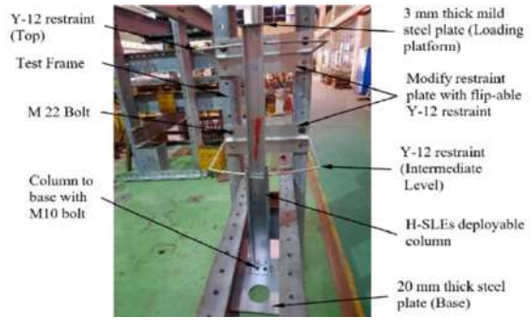

(a) H-SLEs deployable mechanism at vertical configuration

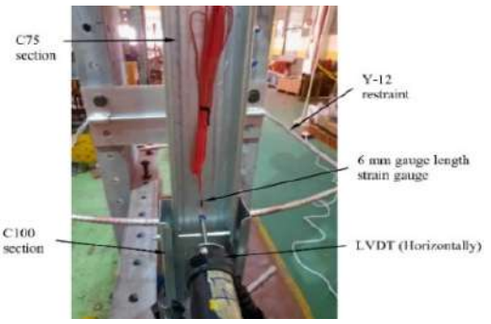

(b) Strain gauge and LVDT (Horizontal direction) position

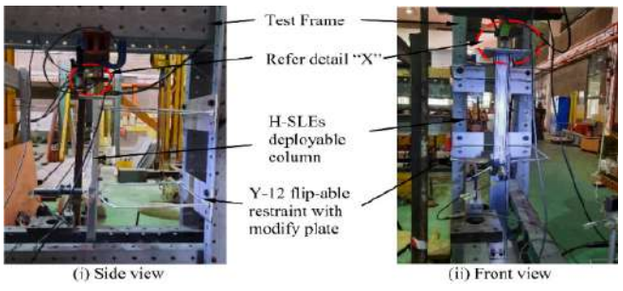

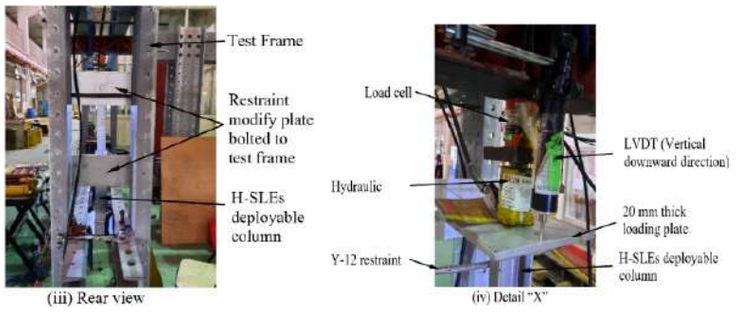

(c)Views of isolated H-SLEs deployable column under load test configuration

FIGURE 2. Load test configuration and apparatus setup view

LOAD TEST PROCEDURES

The initial compression axial load of 0.2 kN (Approximately 10% of total maximum expected design load) was applied to the loading plate to ensure all joints fit and ready to apply loads. Then, the load cell was set back to initial zero to start the actual load test. The applied load was 0.5 kN/ step manually using hydraulic jet. The load applied to the specimen at first considered as dynamic load and will wait for the loads become static load before next load step applied. This static load was recorded together with the displacements (Horizontal and vertical) occurred at the same time in term to determine the structure respond to the loads apply. During load test, the observation also carried out to identify the failure modes occurred to the members and joints. Besides, the first started and further failure point and mode of failure also identify along the load test. The parameters such as maximum load, displacements, member strain, member buckling, bolt capacity and bearing capacity were determined and recorded. The raw data of the load test were recorded in the TDS-7130 software and then analyzed for discussion and finding.

FAILURE MODES

The experimental data obtained was presented in graph and table and the observation results such as failure modes throughout the test was identified and discussed (Figure 3). The results showed that the failure modes observed were bolt bending failure, section buckling failure and bearing failure. The specimens for S1, S2, S3 and S4 were failed at bolt bending failure mode due to small bolt size used (M6 and M8 bolt) between C75 and C100 connection (Figure 3a). This was due to the applied load exceeded bolt capacity and indirectly has pulled the C75 section flange end node deformed at incline position. Besides, the bolt bending failure has led to others failure such as excessive bearing deformation at bolt hole perimeter due to pulled force from bolt bending effect at C100 flange (Figure 3a.i) and section C75 flange bearing failure (Figure 3a.ii). The C75 section end node not fixed to position has made it easy to move or deformed based on bolt bending direction.

The experimental results also indicated that M10 bolt used has reduced the bolt bending effect for specimens S5 and S6 (Figure 3b). The M10 bolt bending at left side has indirectly cause the C75 section flange right side suffered shortening effect due to elongation at left side and has pushed the right-side flange moved to upright position. Besides, the C75 section end node was not fixed and caused section flange end node moved along the bolt hole direction (Figure 3b). At the end, C75 section flange left side will have suffered bearing failure at incline position and right side has buckled due to pushed up effect.

The specimens for S7 and S8 showed that the C75 (0.75 mm thick) section were suffered from buckling effect at mid-span section flange and quarter length measured from the bolt joint (Figure 3c). This was due to C75 section exceeded their capacity but M10 bolt remain strong to sustain the load applied. If the C75 section not shown the adverse deformation at mid-span or others position of the section (Out of section lapping area), the buckling and bearing deformation failures will have occurred at joint lapping area (Figure 3c). Thus, thin section with big bolt size used will caused two failure conditions, that was buckling at mid-span when the bolt size used was strong enough to resist the vertical load applied and mild buckling deformation occurred at mid-span but adverse buckling and bearing failure at end node.

The specimens S9 and S10 results indicated that C75 section (0.75 mm thick) suffered buckling at mid-span area and section end node (Section lapping area in Figure 3d). This indicated that the M8 bolt used able to resist the vertical load applied while for C75 section buckled due to section capacity exceeded. For specimens S11 and S12, the C75 section suffered buckled at mid-span until end node for both specimens. The M6 bolt used for both specimens also suffered bending failure and this failure has indirectly caused the C75 section flange buckled at one side while another side of the C75 section flange remain unchanged for their shape. The bolt bending failure mode has pushed the C75 section upward and caused buckled started from end node until mid-span as showed in Figure 3d.

Based on the observation results obtained, it can be concluded that the H-SLEs deployable mechanism will failed at buckling, section bearing failure and bolt bending failure under compression axial load. The bolt bending failure due to small bolt size will indirectly pulled or pushed the C75 section flange buckled and caused bearing failure at the end node since the C-section end node was not fixed. The thin C75 section will buckled at mid-span of C75 section flange if the suitable bolt size used and presented greater bolt resistance capacity than C75 section capacity. Therefore, thin C-section with suitable bolt size will caused C-section buckling at mid-span but if small bolt size used, it will have caused bolt bending and indirectly impact to the C-section buckled due to pull and push forces from the bolt bending effect.

Besides, the combination of thicker C-section (1 mm thick) with suitable bolt size (M10) sustain more loads compared with combination of thin C-section and small bolt size. Therefore, the relationship between the bolt size used in the connection of H-SLEs deployable mechanism with the structural parameters such as maximum load, displacements and member stresses were summaries as in Table 3.

(a) S1, S2, S3 and S4

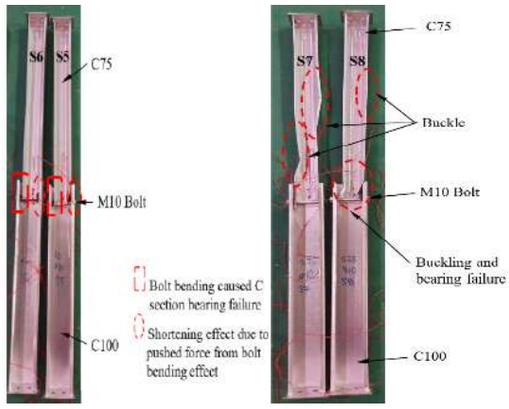

(b) S5 and S6 (c) S7 and S8

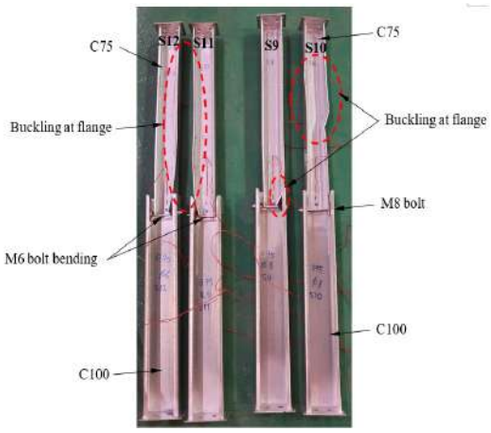

(d) S9, S10, S11 and S12

FIGURE 3. Isolated H-SLEs deployable mechanism failure view

TABLE 3. Relationship between bolt size and structural parameters

Dia. Bolt, mm	P_{max}	Displacement		Stress, σ	Remarks
		Δ_v	Δ_h		
10	High	Small	High	High	High stress in the section members has caused the elastic deformation.
8 6	Low	High	Small	Low	Low stress due to buckling at mid-span disturb the stress distribution to end node. Mild deformation to the members except the bolt hole connection area.

LOAD CAPACITY AND BEARING RESISTANCE

The ultimate load and bearing resistance of isolated H-SLEs deployable mechanism at deployed configuration under compression axial load test results was tabulated in Table 4. The results in Table 4 showed that the highest ultimate load capacity was obtained from M10 bolt connection for both 1 mm and 0.75 mm thick C75 section connection with C100 section. This ultimate load was decreased parallel to the reduction of bolt size used. The M10 bolt connection with 1 mm and 0.75 mm thick C75 section were 10.88 kN (S5 and S6) and 8.77 kN (S7 and S8) respectively. Besides, the M10 bolt connection with 1 mm and 0.75 mm thick C75 section performed closely with BS EN 1993 design bearing resistance ratio, that were 0.88 and 0.95 respectively but for M8 and M6 bolt connection were out of acceptable level.

TABLE 4. Summary of compression axial load test results.

Sam-ple ID	Bolt Dia. (mm)	Height, h (mm)	P_{max} (kN)	Average P_{max} (kN)	BS EN1993 $F_{b, RD}$ (kN)	BS EN1993 $F_{net, RD}$ (kN)	P_{max}/ Bearing Resistance Ratio
S1	M6	1158	7.11	7.17	13.49	11.97	0.53
S2	M6	1158	7.23				
S3	M8	1158	9.86	9.26	13.49	12.21	0.69
S4	M8	1158	8.66				
S5	M10	1158	10.79	10.88	13.49	12.32	0.88
S6	M10	1158	10.98				
S7	M10	1158	8.68	8.77	9.24	9.24	0.95
S8	M10	1158	8.87				
S9	M8	1158	7.53	6.99	9.24	9.16	0.76
S10	M8	1158	6.44				
S11	M6	1158	6.35	6.20	9.24	8.98	0.67
S12	M6	1158	6.06				

The comparison between actual load capacity and BS EN 1993 design bearing resistance were conducted based to their failure modes such as M6 and M8 bolt due to bolt bearing resistance while for M10 bolt due to net section bearing resistance. This was because M6 and M8 bolt suffered from bending failure while for M10 bolt connection, the C-section suffered from bearing and buckling failure. The ultimate load obtained for M10 bolt connection was satisfactory since less than 15% acceptable level but for M6 and M8 bolt connection result were not satisfactory since acceptable range exceeded compared with BS EN 1993 design bearing resistance. Besides, the thin section weakest than thick section in sustaining the compression axial load for H-SLEs deployable mechanism. This scenario can be proved by the ultimate load over bearing resistance ratio where the ratio going up represented the weakest section when section thickness considers for measurement. Therefore, 1 mm thick C75 section produced less ratio compared with 0.75 mm thick section. Therefore, it can be concluded that minimum bolt size used to produce safe and stable H-SLEs deployable mechanism as load bearing compression member was M10 bolt and thicker section will have improved structure strength and stability.

LOAD-DISPLACEMENTS

The structure instability of the H-SLEs deployable mechanism was predicted influence by the parameter horizontal displacement at bolted joint. Horizontal displacement at the bolted connection area between two C-section end node (System restraint point) was the weakness point due to gravity load and applied load will deploy (Fold) the H-SLEs mechanism and lastly caused instability to the structure. Megson (2005) has explained the column buckling theory where the vertical structure element may suddenly bow under compression axial load due to horizontal displacement. Therefore, the H-SLEs deployable mechanism at deployed configuration was behaving as column and the horizontal displacement measured must within the safe limit as recommended by SETO (2000). The overall load-horizontal displacement results obtained for 1 mm and 0.75 mm thick C75 section was showed in Figure 4.

The results obtained in Figure 4 indicated that M10 bolt connection between two C-section sustained highest load and followed by M8 bolt while M6 bolt connection sustained lowest load. The initial to point 1 indicated the resistance of bolt joint against applied load with linear relationship for all three curves (M6, M8 and M10 bolt) where the increment of load has increased the horizontal displacement value. Among these three curves, M6 bolt curve showed the weakest connection with 1.35 mm horizontal displacement while M10 bolt was the strongest connection with the horizontal displacement value of 0.9 mm when load approaching 3.8 kN. The high horizontal displacement value obtained represented the weakest connection where the load applied easier to push the connection and move horizontally compared with low horizontal displacement value.

The H-SLEs deployable mechanism with M6 bolt connection from point 1 to point 2 represented the bearing stage of the bolt with high horizontal displacement value and small applied load. The bolt starts to bend at point 2 and behave as the transition point from positive horizontal displacement direction to reversed direction. At position point 2 to point 3, the reversed direction indicated the bolt suffered from bending has pulled the C75 section at end node to deform because it was not fixed and lastly caused the bearing failure. This has caused the C75 section bowl at web due to two side flanges pulled by bolt bending effect and caused the reversed direction of horizontal displacement. The web bowl condition also can be categorized as distortional buckling effect since the end node (two side C75 section flange) was not fixed and free to move. The C75 section bowl effect at web also caused by the section not thick enough to sustain the load applied and caused high stress to the section web. The specimen with M6 bolt connection failed at ultimate load of 7.13 kN and the horizontal displacement was 1.29 mm (Reversed direction).

The specimens with M8 bolt connection indicated that from point 1 to point 2 represented the bearing stage and start bending at point 2 behave as the transition point from positive horizontal displacement direction to reversed direction. The horizontal displacement from point 2 to point 3 showed the reversed direction where the bolt suffered from bending which caused one side bolt move upward while another side move downward. Thus, the C75 section has twisted where one side move to front and another side move to back and the LVDT has measured the movement for C75 section web moving back direction. The increment of load has caused a pushed back effect to C75 section web, and the horizontal displacement value measured back to original going up trend (point 3 to point 4). When the applied load exceeded 8.94 kN with 4.14 mm horizontal displacement, point 2 to 3 scenarios repeated but with straight slope until ultimate load of 9.15 kN with 3.76 mm horizontal displacement (Reversed direction).

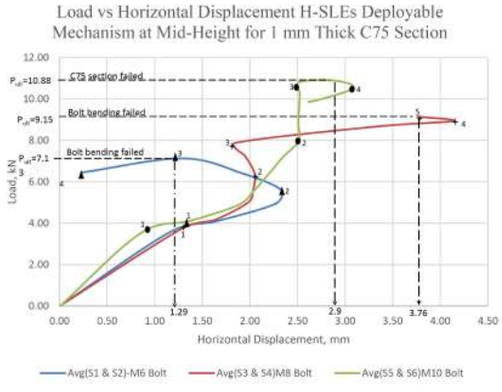

(a) 1 mm thick C75 section

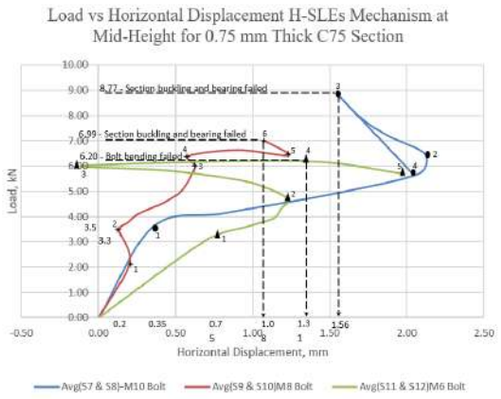

(b) 0.75 mm thick C75 section

FIGURE 4. Load versus horizontal displacements for H-SLEs mechanism

The load-horizontal displacement curve for M10 bolt connection in Figure 4a showed a load proportional to the horizontal displacement value measured. The point 1 to point 2 curves represented the bearing stage where the increment of load applied has increased the horizontal displacement value. The load-horizontal displacement from point 2 to point 3 indicated that more load applied required to cause the horizontal displacement. The further increment of load continuously has exceeded C75 section capacity and lastly failed at section bearing at ultimate load of 10.88 kN with 2.9 mm horizontal displacement.

The overall load-horizontal displacement results along the compression axial load test for H-SLEs deployable mechanism with 0.75 mm thick C75 section was showed in Figure 4b. The results obtained indicated that M10 bolt connection sustained highest load of 8.77 kN with 1.56 mm horizontal displacement, and followed by M8 bolt connection while the M6 bolt connection produced the lowest load, that was 6.20 kN with horizontal displacement of 1.31 mm. The initial point 0 to point 1 for all cases (M6, M8 and M10 bolt) represented the resistance of bolt joint against applied load.

The M10 bolt connection specimen showed the bearing stage from point 1 to point 2 where the increment of load has increased the horizontal displacement proportionally. When the applied load exceeded point 2 value, the C75 section flange was suffered from buckling effect and caused the C75 section pushed the LVDT to reversed direction as represented by point 2 to point 3. At point 3, it was achieved the ultimate load of 8.77 kN with 1.56 mm horizontal displacement and the further increment of load has caused failure to the specimen (Point 3 to point 4).

The specimen with M8 bolt connection indicated that from point 1 to point 2 represented the bearing stage of the C75 section and start to buckle and caused the twisted effect to the C75 section at web (point 1 to point 2) and the horizontal displacement measured indicated the positive horizontal displacement to reversed direction. When the twisted effect at stable state, the increment of load was

proportional to the horizontal displacement as showed in point 2 to point 3. At point 3 to point 4, the twisted effect repeated due to buckling of the C75 section flange. The further increment of load has caused the increased of horizontal displacement (Point 4 to point 5) and lastly, the increment of load has caused the specimen failed at C75 section flange buckling failure with the ultimate load of 6.99 kN with 1.08 mm horizontal displacement.

For M6 bolt connection, the bearing stage occurred from point 1 to point 2 where the increment of load will have increased the horizontal displacement value. Once the applied load reached and exceeded point 2, the C75 section will start buckled and caused the web of the section twisted. This will make the section one side moved to front while another side move to back. The horizontal displacement moved to reverse direction indicated that the C75 section twist effect and caused the web one side move to back as represented from point 2 to point 3. At the same time, the bolt also suffered from bending failure and caused pulled force to pull the C75 section and caused the horizontal displacement at reversed direction. The increment of load has caused the specimen failed at ultimate load of 6.20 kN with horizontal displacement of 1.31 mm. Finally, the specimen also failed at bearing at C75 section end node beside buckling failure at C75 section.

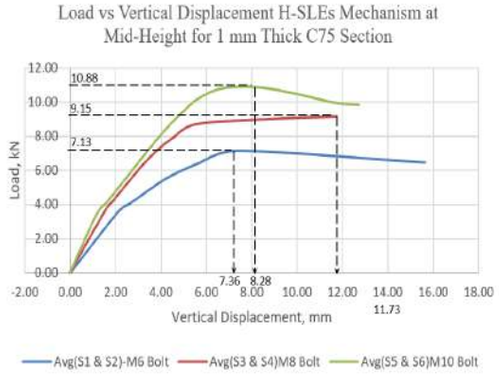

(a) 1 mm thick C75 section

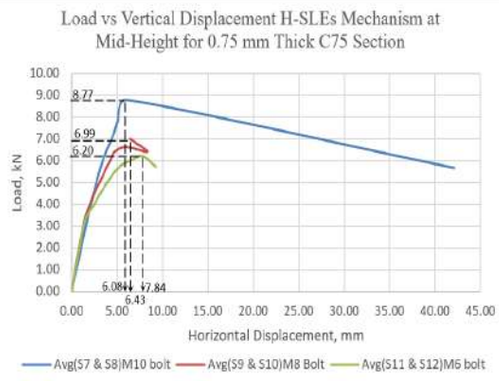

(b) 0.75 mm thick C75 section

FIGURE 5. Load versus vertical displacements

The load-vertical displacement results for 1 mm and 0.75 mm thick C75 section with M6, M8 and M10 bolt connection were showed in Figure 5. The results showed that the vertical displacements were proportional to the load applied. The increment of load will increase the vertical displacement and the load-displacement curves obtained was smooth. The M10 bolt connection sustained highest load of 10.88 kN while the M6 bolt only sustained 7.13 kN. These results obtained was compatible with the predicted results where the big bolt size able to sustain more load and reduced with the decreased of bolt size.

The compression axial load applied will cause the shortening effect to the H-SLEs mechanism C-section and in this case, the bolted connection area between two C-section will displaced horizontally. This will make the connected C-section member (C75) at inclined position due to horizontal displacement at bottom end node and shortening (Vertical downward displacement) at top end node within same applied load value. This scenario was compatible with the analytical result for motion pathway where the vertical displacement values were greater than horizontal displacement values. The compression force applied has caused high vertical displacement value (Shortening) to the C75 section and indirectly caused the H-SLEs deployable mechanism not exactly straight (90°) with certain inclination for C75 section, especially the bolted joint area. If the bolt strong to resist the compression force, the C75 section will deform due to section bearing capacity exceeded such as buckling along C75 section flange and bearing failure at end node (Bolt connection area) and vice-versa, the bolt will have suffered bending failure and indirectly pulled force the C75 section deformed at bottom section end node since the end node not fixed at bolt position. The load-vertical displacement results obtained for 0.75 mm thick C75 section with M6, M8 and M10 bolt connection were showed in Figure 6b. The results obtained showed the similar behaviours with 1 mm thick C75 section with M6, M8 and M10 bolt connection.

Based on the results obtained, it can be concluded that all the specimen's horizontal displacement values were within the SETO (2000) recommended limit, which was under ± 7.72 mm (h/150). The thin section (C75 - 0.75 mm thick) will suffered less horizontal displacement compared with thicker section (C75 – 1 mm thick) since the compression axial load sustained was low. These results obtained was compatible with the theory projected result where thicker section is stronger than thin section in sustaining the compression axial load since thicker section could sustain more load due to bigger section covered area. The load-horizontal displacement curves obtained was not smooth due to cold-formed steel is thin sheet section which will easily to deform subjected to the load path in the section. Therefore, the H-SLEs mechanism constructed by using cold-formed C-section was recommended not used as individual member but used in bundle which can behave as self-bracing system when tie-up together and produce stable structure compared with single H-SLEs mechanism.

The load-displacements results obtained indicated that the vertical displacement value was greater than horizontal displacement value. The results were compatible with the projected result in analytical study where the motion pathway for *x*-axis was less than *y*-axis value. This is because the intersection between horizontal displacement and inclined member will create angle where the big angle will reduce the total load sustained and vice-versa. The higher the horizontal displacement value indicated that the H-SLEs deployable mechanism less stiff in sustaining applied load and vice-versa. The lateral stability of the H-SLEs deployable mechanism was highly dependent to the horizontal displacement value and must not exceeded the recommended limit of h/150 as proposed by SETO (2000). Therefore, it can be concluded that the horizontal displacement will dominate the maximum load sustain due to angle created with incline member and H-SLEs mechanism stability due to lateral movement.

MEMBER STRAIN

The member strain refers to the cold-formed steel section deformation under compression axial load either in tension or compression. The deformation of member due to stress can be categorized into two, that are either elastic or plastic deformation. The member stress in this case will focus on the C75 section end node at bolted connection area since the C75 section end node does not fix and free to move and deform. The results obtained in Figure 6 showed the plastic deformation for all specimens due to stress and not embracing sustainability approach.

The results in Figure 6a showed the H-SLEs deployable mechanism with M6 bolt connection specimens has caused highest stress to the C75 section compared with M10 and M8 bolt connection specimens. The M6 bolt connection will caused the critical deformation to the C75 section where the bolt bending failure has pulled the section end node deformed and increased the C75 section stress due to pulled forced from the bolt bending effect. While for M8 bolt specimen, the lowest stress obtained compared with M6 and M10 bolt connection specimens. This happened due to the mild bolt bending effect to the C75 end node and the member stress has started to reduce from 41.9 N/mm^2 at load of 8.67 kN. At this moment, the stress in C75 section was reduced accordingly because the section at plastic zone and the increment of applied load at this stage has more impact to the bolt. Therefore, the increment of applied load after load of 8.67 kN has reduced the C75 section stress but impact the bolt which finally caused bolt bending failure to the specimen connection. Besides, this scenario also indirectly caused C75 section bearing failure at the end node (Bolted connection lapping area).

The M10 bolt connection produced lowest stress in C75 section due to stronger bolt capacity in resisting compression axial load and no bolt bending effect happened to create additional stress to C75 section. For 0.75 mm thick C75 section, the applied load has caused less stress to the section since the load sustain was less compared with 1 mm thick C75 section due to the 0.75 mm thick section effective area is less than 1 mm thick section effective area. Besides, the big bolt size will produce less stress with high load sustain compare with small bolt size with less load sustained. This was due to the load applied has transfer to the bolt and reduce the C75 section stress compared with small bolt size where the bolt failure has cause additional stress to the C75 section.

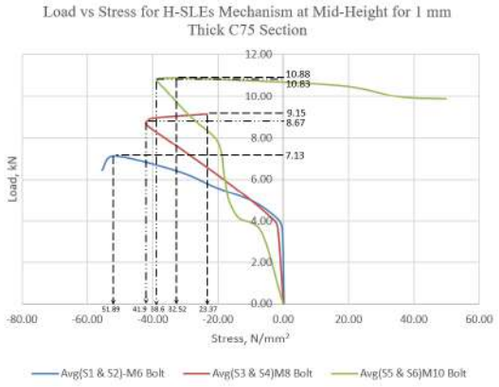

(a) 1 mm thick C75 section

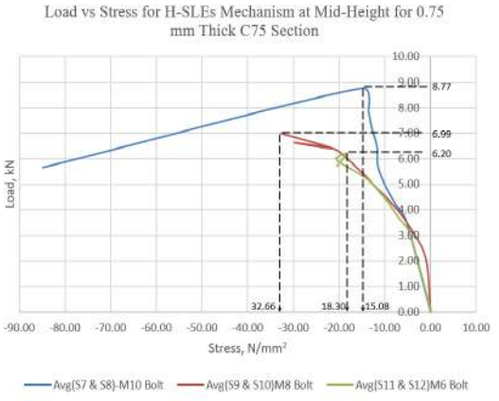

(b) 0.75 mm thick C75 section

FIGURE 6. Load versus stress

Therefore, it can be concluded that the section thickness will impact the member stress where the thicker section will produce more stress since their covered area for the load sustained was high compared with thin section. Besides, the suitable bolt size used also will impact the C75 section stress where the small bolt size used has produced high stress in the member compared with big bolt size. In addition, the small bolt size used has indirectly increase the C75 section stress due to bolt bending effect has pulled the C-section to deform. The stresses occurred has caused plastic deformation to C-section. Thus, the designer must take note for this either design for elastic or plastic deformation due to stress. When the design is in elastic range, the ultimate load sustain will reduce and if design at plastic range, the ultimate load will high and not be embracing sustainability principle.

CONCLUSION

An experimental study was conducted to investigate the isolated H-SLEs deployable mechanism performance under compression axial load. The finding indicated that big bolt size used will have produced high ultimate load capacity, horizontal displacement, and member stresses but small vertical displacement and vice-versa behaviors for small bolt size used. Suitable section dimension and bolt size used are importance combination in developing the stable and stiff prefab H-SLEs deployable mechanism. The H-SLEs deployable mechanism constructed by using cold-formed C-section was recommended not used as individual member but in bundle for self-bracing purposes and improve C-section stiffness such as bamboo stiffness arrangement to resist twisting effect during load applied. High member stresses measured for the thin section and small bolt size combination due to bolt bending effect.

Based on the experimental results obtained, the bolt bending failure was the most critical parameter for isolated H-SLEs deployable mechanism. Besides, the M10 bolt connection with 1 mm and 0.75 mm thick C75 section connection performed closely with BS EN 1993-1-1 and BS EN 1993-1-3 design bearing resistance ratio and satisfactory since less than 15% acceptable level. While for M8 and M6 bolt connection for differences C75 thick section was not satisfactory because 15% acceptable level exceeded. Thus, it is recommended that M10 bolt use as minimum requirement in fabricating H-SLEs deployable mechanism using cold-formed steel.

ACKNOWLEDGEMENT

The authors would like to thank Politeknik Sultan Idris Shah and Universiti Teknologi Malaysia for their support of laboratory facilities to complete this research.

DECLARATION OF COMPETING INTEREST

None

REFERENCES

Andrea, E. D. G., & Paolo, B. 2013. Deployable structures. *Advance Science & Technology* 83: 122-131.

British Standards Institution. 2005. BS EN 1993: Part 1- 1: Design of steel structures- General rules and rules for buildings. UK.British Standards Institution. 2006. BS EN 1993: Part 1-3: Design of steel structures- General rules – Supplementary rules for cold-formed members and sheeting. UK. British Standards Institution. 2005. BS EN 1993: Part 1- 8: Design of steel structures- Design of joints. UK.

Esther, R. A. 2015. *Deployable Structures*. Laurence King Publishing Ltd: UK.

Friedman, N., & Ibrahimbegovic, A. 2013. Overview of highly flexible, deployable lattice structures used in architecture and civil engineering undergoing large displacements. *YBL Journal of Built Environment* 1(1): 85 – 103.

Gantes, C., Jerome, J. C., Robert, D. L., & Yechiel, R. 1989. Structural analysis and design of deployable structures. *Computer & Structure* 32:(3/4): 661 – 669.

Hu, H. Y., Tian, Q., Zhang, W., Jin, D., Hu, G., & Song. Y. 2013. Nonlinear Dynamics and Control of Large Deployable Space Structures Composed of Trusses and Meshes. *Advance in Mechanics* 43(4): 390-414.

Kwan, A. S. K., You, Z., & Pellegrino, S. 1993. Active and passive cable elements in deployable/ retractable masts. *International Journal of Space Structure,* 8: 29 – 40.

Li B., Wang S. M., Zhi C. J., Xue X. Z., & Viliam M. 2017. Analytical and numerical study of the buckling of planar linear array deployable structures based on scissor-like element under its own weight. *Mechanical Systems and Signal Processing* 83: 474 – 488.

Maden, F., Korkmaz, K., & Akgu, Y. 2011. A review of planar scissor structural mechanisms: geometric principles and design methods. *Architectural Science Review* 54 (3): 246 – 257.

Megson, T. H. G. 2005. *Structural and Stress Analysis.* Elsevier Ltd: United Kingdom.

Raskin, I., & Roorda, J. 1999. Nonlinear analysis of uniform pantographic columns in compression. *Journal of Engineering Mechanics* 125(12): 1344 – 1348.

Roovers, K., & Temmerman, N. D. 2017. Deployable scissor grids consisting of translational units. *International Journal of Solids & Structure*. 000: 1–17.

Tagawa, H., Sugiura, N., & Kodoma, S. 2015. Structural Analysis of Deployable Structure with Scissor-like-element in Architectural Design Class. *IABSE Symposium Report*.

The Institution of Structural Engineers & The Institution od Civil Engineers. 2000. Manual for the design of steelwork building structures to EC3. SETO: London.

You, Z., & Pellegrino, S. 1997. Foldable bar structures. *International Journal of Solids and Structures* 34(15): 1825-1847.

Zhao, Z. W., Hu, W. B., & Yu, L. 2020. Experimental and numerical studies on the deployment process of self-locking cuboid foldable structural units. *Advances in Structural Engineering* 00(0): 1–13.